

## Astrometry with the Advanced Camera: PSFs and Distortion in the WFC and HRC

Jay Anderson

*Department of Physics and Astronomy MS-108, Rice University, Houston TX 77005*

**Abstract.** Before ACS can be useful for astrometry, we must first determine how best to model the PSF and how to correct for the camera's considerable distortion. I analyze WFC and HRC images taken of the core of 47 Tuc and find that the same effective-PSF-based approach that works for WFPC2 produces excellent results with ACS. Positions of reasonably bright stars can be measured with a random error of better than 0.01 pixel in each coordinate. Distortion is another matter. It is well known that the Advanced Camera for Surveys suffers from significant linear and higher-order distortion. I find that the ACS also suffers from some fine-scale distortion that appears to be different for each filter. This fine-scale distortion perturbs a polynomial solution by about 0.05 pixel and is coherent on spatial scales of about 200 pixels. I find that the distortion in each chip can be modeled with a 4th-order polynomial and a separate look-up table for each filter. With such a model, the distortion residuals are typically  $\sim 0.01$  pixel.

### 1. Introduction

We have found in our research with WFPC2 (see references by Anderson & King) that the two keys to high-precision astrometry with *HST* are (1) careful treatment of the undersampled point-spread function (PSF) and (2) accurate modeling of the geometric distortion. Once these two issues are addressed, it is possible to attain differential astrometry to a fraction of a milli-arcsecond in a well-dithered set of images.

With its large field of view and better sampling, the Advanced Camera for Surveys has the potential to measure positions at least a factor of two better than WFPC2. However, before we can realize this potential we must first learn how to model the PSF and remove the distortion in this new camera.

With regards to the PSF, I have examined some of the early ACS images and find that the same modeling techniques that worked for WFPC2 work quite well for ACS. In fact, in many ways, the ACS PSF is better behaved than that for WFPC2.

It was well known that distortion in the Advanced Camera for Surveys would be much greater than that in WFPC2 (50 pixels as compared with 5 pixels). It was not known how accurately this distortion could be modeled and removed. I have examined several of the data sets available at the center of 47 Tuc and characterized the various sources of distortion present in the two cameras. I find that in addition to the expected large geometric distortion, there appears to be some unexpected component of distortion that is introduced by the filter itself.

### 2. Available Data Sets

There are two main data sets available to explore the PSF and distortion properties in the WFC and the HRC: GO-9028 (PI Meurer) and GO-9443 (PI King). These two sets

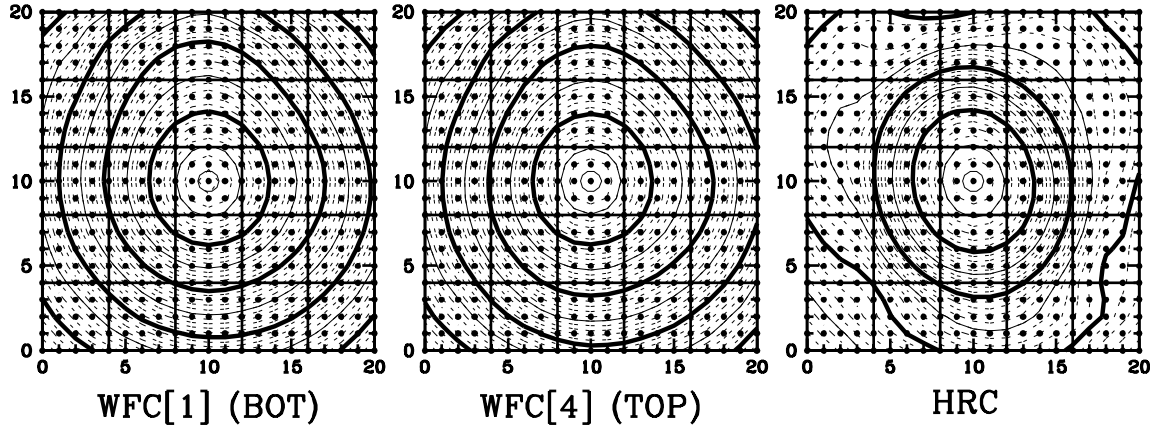


Figure 1. Contour plots of the super-sampled F475W PSFs. These PSFs represent the inner  $5 \times 5$  pixels of a star and are sampled every 0.25 pixel in  $x$  and  $y$ . The heavy contours are separated by 0.5 dex.

were both taken at the center of globular cluster 47 Tuc. The main set (9028) consists of 20 exposures through F475W with a range of offsets all at the same orientation. GO-9443 contains a tightly dithered set of pointings through the same filter at an orthogonal orientation. This program also has several single exposures taken through other filters to allow us to investigate how the solution may vary with filter.

Other data sets cover the same field and an outer field of the same cluster, and will provide valuable checks on the solution.

### 3. The PSF

#### 3.1. Lessons from WFPC2

Our experience with WFPC2 (Anderson & King 2000) has shown us that the main sources of PSF-related astrometric error are due to undersampling and spatial variability. The undersampled nature of *HST* images does not mean that we cannot measure accurate positions for stars, but it does mean that the accuracy of our positions will depend critically on our model of the PSF.

We deal with the undersampling by taking several observations of the same star field with a variety of sub-pixel offsets. This dithered set allows us to reconstruct a properly sampled version of the PSF. Our PSF model is typically super-sampled by a factor of four with respect to the image pixels. We find that without such a carefully constructed PSF, position measurements contain systematic errors of up to 0.05 pixel. But with an accurate PSF model, it is possible to measure positions with a random accuracy of 0.02 pixel and no significant systematic errors.

The WFPC2 PSF changes shape with location in the field, so we derive a different PSF for nine fiducial points in each chip. We interpolate among these fiducial PSFs to construct a PSF that is appropriate for the location of each star we measure.

#### 3.2. ACS Results

I constructed a PSF for the Advanced Camera for Surveys using the same techniques as above for WFPC2. To start, I found a single PSF for each chip. These PSFs are shown in Figure 1. (Note that the images used were the `_flt` or `_crj` images, not the `_drz` images; the latter images are not well suited for astrometry as they have been re-sampled and much of the positional information has been blurred out.)

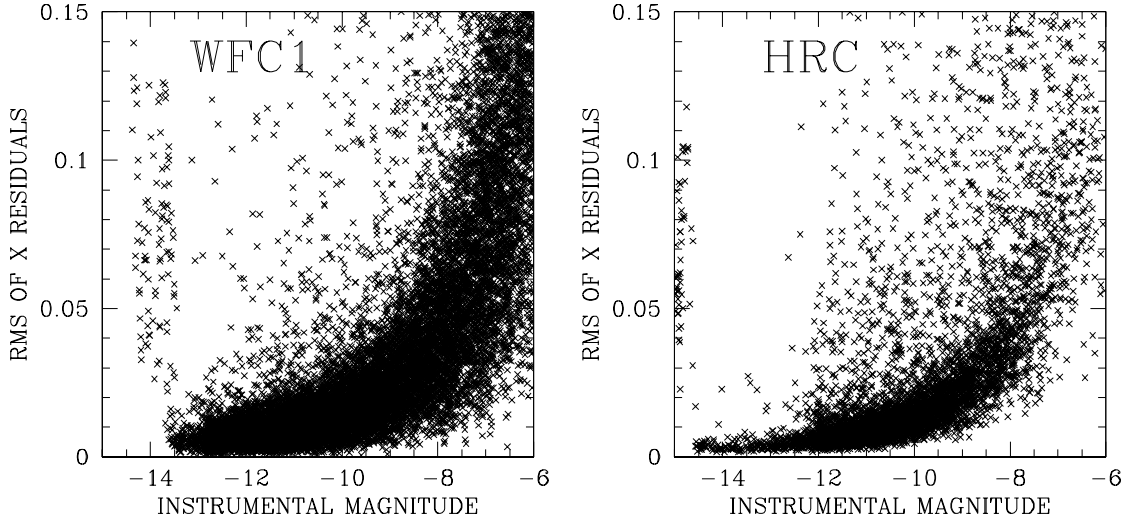


Figure 2. The single-coordinate astrometric precision as a function of instrumental magnitude,  $-2.5 \cdot \log_{10}(\text{DN})$ . Stars brighter than  $-13.5$  in the WFC and  $-14.5$  in the HRC are saturated and have greatly increased errors.

*Astrometric Accuracy.* I find that the  $4\times$ -supersampled PSF model can measure reasonably bright, isolated stars with a random accuracy of better than 0.01 pixel in each coordinate and with no significant systematic errors (see Figure 2). This accuracy with respect to the pixel grid holds true for the WFC and the HRC, so that the HRC angular precision is a factor of two better than in the WFC.

Thus far, I have used the same  $5 \times 5$ -pixel PSF model as we used for WFPC2. Since even in the HRC most of the flux is contained within this aperture, photometry and astrometry should not require a larger-format PSF. However, if one wants to do PSF subtraction, a larger-format PSF might be useful.

*Spatial Variation of the PSF.* The WFPC2 PSF changes shape appreciably from the center of the chip to the corners. We found that if we didn't adequately model the PSF variation, we saw systematic errors in astrometry that correlated with the pixel phase of the star being measured. I therefore examined the astrometric residuals from different regions of the ACS chips in search of such tell-tale signs that the PSF was changing. I found only a very slight (0.002 pixel) hint of this effect in the very corner of the WFC chips. This is a factor of five less variation than was seen across the (smaller) WFPC2 chips. For almost all ACS projects, it should therefore be safe to use a spatially constant PSF—a welcome simplification.

The random accuracy shown above is a factor of two better than we have been able to achieve for WFPC2. This improvement is a result of several factors: (1) we only need to solve for a single PSF over a much larger area, so we have many more PSF samplings from which we can construct a model; (2) the deeper CCD wells make each observed sampling of the PSF more accurate; and (3) the deeper wells also give the bright stars much higher signal-to-noise so that we can fit for a more accurate position.

*Photometric Accuracy.* While my focus has been more on astrometry than photometry, I have examined the photometric residuals as well and find that the best stars can be measured differentially to about 0.005 magnitude in each exposure. However there do appear to be some small systematic errors ( $\sim 0.003$  mag) related to intra-pixel sensitivity variations. In the PSF constructed above, I constrained the pixel-response function to be flat, but more

realistic constraints should be possible once we have better observations of the intra-pixel sensitivity function for the various filters.

*Stability of the PSF over Time.* Finally, I looked at how the PSF changes over the long-term. I measured the GO-9443 images (taken in July 2002) with the PSF from the GO-9028 images (taken in April 2002) and found that the systematic position errors incurred were on the order of 0.005 pixel. This error is a factor of five smaller than we found with a similar WFPC2 comparison (Anderson & King 1999).

This apparent stability of the PSF should be confirmed with additional observations, but if the PSF is typically this stable, then it would be worthwhile to construct a library of PSFs, one for each filter/chip combination. The single-pointing observations of GO-9443 will allow us to find a preliminary PSF for several filters. However to get the best possible PSFs, and to constrain the pixel-response function for each filter, we will need more observations. A tightly dithered set of observations through each filter of a reasonably dense star field should allow us to constrain the pixel-response function and develop an exquisitely accurate PSF for each filter. This would require about an orbit per filter.

*PSF Summary.* The raw astrometric quality of these early ACS images is extremely encouraging. If this precision can be matched with an equally good distortion solution, then the Advanced Camera for Surveys will open up many new avenues for astrometry.

## 4. Distortion

### 4.1. Different Needs

Different applications make different demands on a distortion solution. The pipeline requires a solution that is accurate to about 0.2 pixel, so that the drizzle procedure can create a rectified image that can be easily compared with undistorted images. The solution does not need to be more accurate than this because the resampling inherent in the drizzling process introduces errors of about this size. For this reason, the spec demanded of the initial distortion solution was  $\sim 0.2$  pixel.

Applications which produce a mosaic from a set of offset pointings (perhaps to cover the gap between the chips or to panel-image a large field) are particularly sensitive to distortion errors at the edges of the chips. Such errors can produce additional blurring in the interface-region, resulting in a variation of the resolution with location in the mosaic. Sometimes polynomial solutions can have their largest errors at the edges, so for these applications it may be worthwhile to use a more elaborate solution.

To do differential astrometry, we need to measure relative positions of nearby stars to better than 0.01 pixel. For this, we do not need a solution that is globally accurate at this precision (namely, knowledge of precisely where a pixel in one corner of an image is relative to the pixel in an opposite corner); but we do have to trust that the solution is locally *flat* to very high precision.

Fortunately *all* applications will benefit from the best possible distortion solution on both local and global scales. Thus, our focus has been to examine all sources of distortion, large-scale and small-scale, so that we would arrive at the best possible model for all applications.

### 4.2. How to Solve for Distortion

The easy way to solve for distortion is to observe an astrometrically-calibrated star field with the detector. The detector distortion then shows up directly as position residuals. Unfortunately, there do not exist any astrometric-standard fields with the precision and density that would be useful to help us calibrate *HST*. Hopefully by the end of the ACS calibration procedure the core of 47 Tuc will be able to serve such a purpose.

The hard way to solve for distortion is to do a self-calibration. Here, we observe the same star field through the same detector at various offsets and orientations. We then relate the images to each other, solving simultaneously for the transformations between the images and the distortion. (Usually the telescope pointing is not precise enough to allow us to take the offsets between the images as known.)

### 4.3. Lessons from WFPC2

We have recently completed a new self-calibration of the distortion in WFPC2 (see Anderson & King 2003). While WFPC2 and ACS are different instruments, many of the issues involved in self-calibration will be applicable here as well. Some issues we uncovered in our work with WFPC2 are:

1. In order to solve for distortion, we obviously need observations of the same field at different offsets. If these offsets are too large, however, it can be very difficult to tease apart the solution for the offsets between the pointings from the solution for the distortion itself. It is easiest to use only image pairs with at least 50% overlap.
2. We have found that there are several aspects to a distortion solution: periodic irregularities in the detector, a polynomial solution, variations with focus and filter, additional effects near the chip-edges, the inter-chip solution, etc. It can be extremely hard to solve for all aspects of the solution at once, thus it is useful to examine data sets which can isolate one or two of these effects, and then construct a piecemeal solution that includes all of the effects.
3. The only way to solve for the linear terms is to observe the same field at different orientations. However, if the two observations do not have enough overlap, then the solved-for linear terms are very sensitive to errors in the higher-order terms. In general, the low-order terms are harder to solve for than the higher-order ones, since a global solution can only be as accurate as the local solution.
4. Finally, changes in focus can introduce additional distortions, so that the solution may change over time, both long-term and short-term.

### 4.4. Starting with the WFC

With all these cautions in mind, I began to examine the ACS distortion. I started with the GO-9028 data set, which consists of 20 exposures taken through F475W, with a variety of offsets but all with essentially the same orientation. Such a set of parallel displacements will not allow us to solve for the linear terms, but it is an excellent opportunity to isolate the higher-order terms.

I used the PSFs from the previous section to measure every star in every image. I then cross-identified all the stars in all the images, creating a master list of all the stars in the field and recording the observed location for each star in each image. (This initial task of cross-identification is not easy with images that suffer from as much distortion as ACS!)

*The Polynomial Solution.* The first task is to find the best 4th-order solution. This requires many iterations between determining the inter-image offsets and solving for the distortion itself. In this initial polynomial solution, I set the linear terms to be zero, since we know that parallel displacements cannot constrain them. I found a 4th-order solution very similar to what Meurer et al. (2003) have found: The WFC non-linear terms have an amplitude of about 50 pixels (from center to edge). The HRC non-linear distortion amounts to about 3 pixels in amplitude.

Like Meurer et al., I also found that there are some systematic residuals from this simple polynomial solution. These systematic residuals are typically 0.05 pixel in amplitude and

are coherent on a spatial scale of about 200 pixels. It is clear that we must somehow treat this fine-scale distortion if we desire to make use of the 0.01-pixel precision that is possible with the ACS PSF.

*The Supplementary Look-up Table.* It was surprising to find such fine-scale structure in the solution. The WFPC2 solution had no such fine-scale variation and was almost perfectly fit with a 3rd-order polynomial. It was not practical to model this with a polynomial of even higher order, so I decided to model the additional distortion by means of a supplemental table, sampled every 64 pixels in the WFC ( $65 \times 33$  entries for each chip) and every 16 pixels in the HRC ( $65 \times 65$  entries). To evaluate the distortion at any point in a chip, I interpolate this table and add the table result to the polynomial solution to get the total distortion correction. Solving for the table is also an iterative procedure, and after each iteration I constrain the table to be smooth by convolving it with a  $5 \times 5$  quadratic smoothing kernel. The table for the bottom WFC chip is shown graphically in Figure 3.

The residuals from this polynomial-plus-table solution are typically less than 0.01 pixel, both for the HRC and for the WFC. There remains some quasi-periodic high-frequency variation with a scale of  $\sim 120$  pixels and with an amplitude of about 0.005 pixel. This is likely due to limitations in the look-up table formulation. The smoothing I perform means that the table cannot correct for variations on a scale smaller than about 150 pixels. Improving the distortion solution further may require observations with an array of dither offsets that are better spaced to sample the distortion at this spatial frequency.

*Inter-chip Solution.* The gap between the WFC chips is qualitatively different from the gap between the WFPC2 chips. Each of the WFPC2 chips is independently imaged by different optics, whereas the ACS/WFC chips are all in a common image field and the gap is simply a physical offset between the chips. This offset should not change with time and breathing as much as the WFPC2 offsets do, so it should be safer to use a meta-chip solution for the WFC. The meta-chip solution is included as part of my standard distortion correction. The errors in the inter-chip solution appear to be no larger than those in the global single-chip solutions.

*Distortion from Detector Defects.* Because of a manufacturing defect, every 34th row in WFPC2 is slightly (3%) narrower than average. This was noticed early-on in the flat fields, but it was not initially known if it was a geometric effect or a pixel-sensitivity effect (Holtzman et al. 1995). We demonstrate in Anderson & King (1999) that it is indeed a geometric effect—it produces a 0.03-pixel skip every  $\sim 34$  pixels. We provide a simple correction for this.

The WFC flat fields are seen to exhibit a similar striping every  $\sim 68$  columns, so I looked for an astrometric signature here as well. I plotted the localized relative intensity of the flat field as a function of column number (see Figure 4) and noticed not only a bright column, but a regular pattern with an rms amplitude of 0.1% and maximum amplitude of 0.8%. The expected astrometric signature of this is 0.008 pixel, four times smaller than with WFPC2. Nonetheless, I examined the position residuals as a function of this 68.270-column phase and, sure enough, the observed trend matched up almost exactly with the predictions based on the flat fields. It should be relatively straightforward to come up with a correction for this; but since it is a small effect, I will put off deriving a correction until the other (larger) sources of distortion are properly treated.

#### 4.5. Comparing with the GO-9443 data set

In a self-calibrated solution, we need to have at least one pointing that is rotated with respect to the others in order to solve for the linear terms. That was the idea behind taking GO-9443 with an orthogonal orientation to the many GO-9028 images.

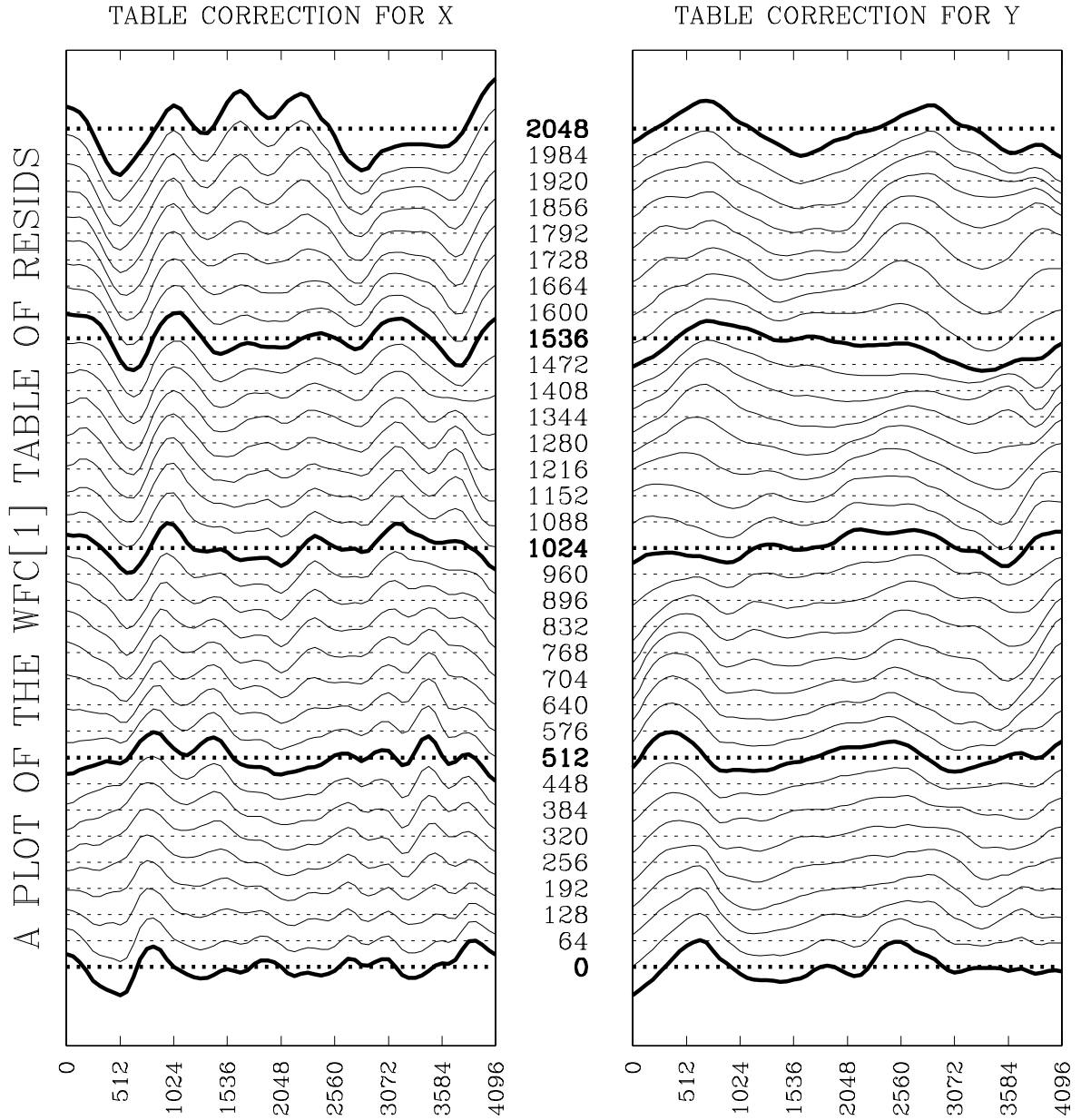


Figure 3. Graphical presentation of the WFC[1] (bottom chip) table of corrections. I plot each of the 33 rows along with its baseline. The  $y$  coordinate corresponding to the center of each row is labeled up the middle. The separation between rows is 0.05 pixel. The table corrections are generally smaller than 0.05 pixel, but can be larger than 0.1 pixel.

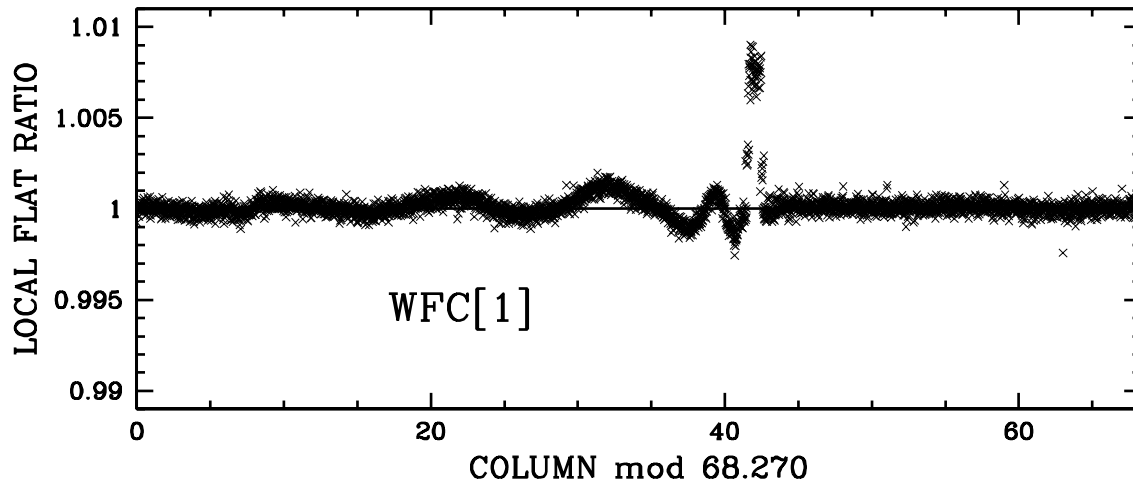


Figure 4. For each pixel in the WFC[1] flat, I took the ratio of the pixel value to the median of the 30 pixel values on either side. I then took a median of this ratio for all 2048 pixels in each column. This is plotted for each of the 4096 columns in a phase diagram.

*Introducing the Orthogonal Pointing.* In my initial attempt to solve for the distortion, I took the orthogonal pointing of GO-9443 and compared it against the twenty GO-9028 pointings, thinking that would allow me to solve for the linear *and* the higher-order distortion at the same time.

Using the residuals from these 1-versus-20 image comparisons, I found a solution which did a very good job reducing the residuals. But when I used this solution to compare the 20 GO-9028 pointings with each other, I found significant systematic residuals. This indicated that there was some change in the solution between the two observations. So, I decided to focus first on the non-linear terms (as above) using exclusively the parallel GO-9028 observations, and only later compared with the orthogonal pointing.

*Comparing with the Orthogonal Pointing.* I correct both the GO-9028 and orthogonal GO-9443 observations with the above polynomial-plus-table solution and examine the residuals between the two sets of positions. The most obvious difference comes from the whopping linear terms, which of course have not yet been solved for. These linear terms correspond to a shear of over 500 pixels from bottom to top in the WFC field.

Once the linear terms are solved for and removed, however, I find that the positions in the two frames still do not match up perfectly, indicating that there is some distortion that has not been removed. In fact the non-linear distortion difference between the two images appears to be almost entirely *quadratic*. Figure 5 shows the position residuals between the GO-9443 and GO-9028 observations.

Note that this smooth behavior would be impossible to see without an exquisite high-order solution. If we had left out the fine-tuning tabular portion of the solution, the quadratic behavior would be completely washed out by the interplay of the fine-scale distortions in the two images being compared. Also, if we had not bundled the two chips together but had transformed them separately, then the quadratic behavior would have been much harder to see—much of it would be absorbed in the fit for the linear terms in the four half-chip overlaps.

The smoothness of this relationship means that the high-order and fine-scale solutions are essentially *constant* over time. The residuals are even continuous across the chip gaps ( $Y \sim 2048$ ), which means that the inter-chip solution is extremely stable as well. Only the

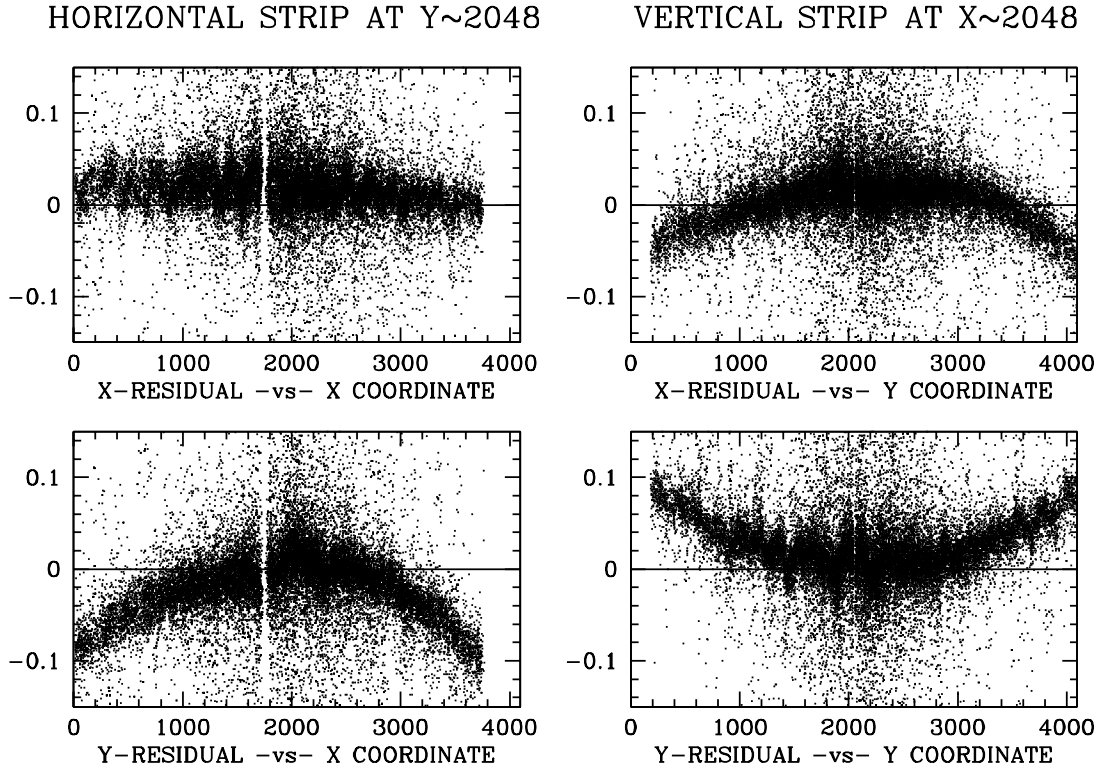


Figure 5. The position residuals between the central GO-9028 pointing and the orthogonal GO-9443 pointing for horizontal (left) and vertical (right) strips through the center of the image. The high-frequency striping is likely related to the smoothing length of the table solution.

low-order terms appear to change with time. (We should note that we cannot rule out a variation of the linear terms of the solution along with the quadratic. Since we had to use these observations to constrain the linear terms, we cannot detect a change in the linear terms.)

This observed quadratic variation is probably due to changes in focus. It should not constitute a major limitation to WFC astrometry. However, it will force us either to use more local transformations or to transform with 2nd-order rather than linear transformations.

*Variation of the Solution with Filter.* The GO-9443 data set had a dithered set of images taken through F475W (the filter that was chosen for the initial distortion mapping), but also had several single exposures at the same pointing through different filters: F435W, F555W, F606W, and F814W. By comparing the positions in the F475W images with the positions measured for the other filters, we can see how much the distortion solution varies with filter.

Whereas in WFPC2, the image-scale had a strong correlation with filter wavelength, the ACS filters all seem to have the same global solution. The different filters do have different fine-scale solutions, however, which will require a separate look-up table for each filter. This is the case for both the WFC and the HRC. Without treatment of the filter-dependence, the distortion solution will only be accurate to 0.1 pixel or so.

(While it is true in general that the different filters share the same backbone polynomial solution and do not have markedly different scales, it is worth noting that F814W images

do seem to have a slightly different scale than the other filters, amounting to almost a half pixel from top to bottom of the WFC. This is accounted for in my F814W look-up table supplement, and could be important for those programs that need to create co-registered mosaics for a variety of filters.)

*An Independent Check.* The program of GO-9018 (PI De Marchi) images an intermediate field in 47 Tuc with the WFC. The program was taken to study the accuracy of the low-frequency flat fields and consists of several pointings with large offsets through a variety of filters.

While the star density in this outer field is not high enough to constrain the distortion solution, there are enough stars in the images to allow us to test the solution. I compared the distortion-corrected star positions in images taken at different offsets and through different filters and found that the systematic position residuals are generally less than 0.01 pixel, which demonstrates that the filter-specific distortion corrections are indeed good to about this accuracy. Evidently, the breathing-state of the telescope during GO-9018 was similar to that during the GO-9028 observations, since no variation of the solution is seen here.

GO-9019 (PI Bohlin) has re-observed the center of 47 Tuc with the HRC in a program analogous to GO-9018. This data set will provide a valuable check on the HRC solution.

## 5. Recommendations

There are many aspects to the ACS distortion solution: a polynomial backbone, a fine-scale solution, a dependence on filter, and a low-order variation with breathing. Not all of these aspects will be of concern to all observers. Many applications require a solution which is accurate to only 0.1 or 0.2 pixel, so that basic image rectification and reconstruction can be done. The polynomial solution produced by Meurer et al. should be entirely adequate for these purposes. Other applications, such as high-precision differential astrometry or careful mosaicking, may require a more elaborate solution, such as the one I have constructed here.

## 6. End-products of this Analysis

This analysis will produce several products that could be useful to the community. Thus far, I have created a FORTRAN subroutine that computes the WFC distortion correction for the five filters in GO-9443: F435W, F475W, F555W, F606W, and F814W. This routine can be downloaded from my anon-ftp site (<ftp://cusp.berkeley.edu/pub/jay/ACS>).

Additional products of this analysis will be: the HRC corrections, PSFs for a variety of ACS filters, and a list of  $\sim 150,000$  stars at the center of 47 Tuc with coordinates in a distortion-free system, so that in the future distortion corrections can be done the easy way.

**Acknowledgments.** This research was supported by STScI grant GO-9443.

## References

- Anderson, J. & King, I. R. 1999, *PASP*, 111, 1095  
 Anderson, J. & King, I. R. 2000, *PASP*, 112, 1360  
 Anderson, J. & King, I. R. 2003, *PASP*, (in press)  
 Holtzman, J. A., Burrows, C. J., Casertano, S., Hester, J. J., Trauger, J. T., Watson, A. M., & Worthey, G. 1995, *PASP*, 107, 1065  
 Meurer, G., Blakeslee, J., Lindler, D., & Cox, C. 2003, this volume, 65